Notes

Reaction Temperature Dependent Formations of the Zero- and One-Dimensional ZnS:Mn Nanocrystals

Young-Ah Kim and Cheong-Soo Hwang*

Department of Chemistry, Institute of Nanosensor and Biotechnology, Dankook University, Yongin, Gyonggi 448-701, Korea
**E-mail: cshwang@dankook.ac.kr*
Received September 6, 2007

Key Words : ZnS:Mn nanocrystal. Nano rod and dot mixture. Temperature dependent shape formation

Low dimensional semiconductor nanocrysals have attracted considerable interest over the past few decades.[1] These materials exhibit unique chemical and physical properties that can be applied to non-linear optics[2] or electronic devices,[3] and more recently to some advanced biotechnology areas.[4] There has been considerable progress in the methods for preparing semiconductor nanocrystals including gas, solid, and aqueous solution phase reactions at various temperatures and pressures.[5] In addition, recent studies have shown that the size and shapes of low dimensional nanocrystals can be tuned by controlling the reaction conditions, such as the concentration of precursor materials as well as the nucleation and crystal growth temperature.[6]

ZnS:Mn nanocrystals have attracted particular interest on account of their high photoluminescence efficiency and stability at ambient temperature, which are properties essential for commercial electro-luminescence devices.[7] This study examined the unique optical and magnetic properties of the ZnS:Mn nanocrystals as a potential candidate for an optical or a magnetic probe in biomedical imaging. Previously, various amino acid ligands capped water-dispersible ZnS:Mn nanocrystals were synthesized.[8] This paper reports the formation of zero- (dot) and one-dimensional (rod) hydrophobic ZnS:Mn nanocrystals under different reaction temperatures along with their characterization.

Experimental

A mixture of 2.0 mL of 0.1 M Et_2Zn (2 mmol) and 0.42 mL of $(TMS)_2S$ (2 mmol) in TOP (tri-n-octylphosphine) solvent was added drop wise to a flask containing bis(acetylacetonato)manganese (II) (0.01 g, 0.04 mmol) in 25 mL of a TOP/TOPO (tri-*n*-octylphosphine oxide) solvent mixture at four reaction temperatures, 50, 100, 135 and 150 °C respectively. After stirring for 30 minutes at the particular reaction temperature, the resulting solutions were cooled to *ca.* 90 °C and incubated for 10 hours. An exception was made for the mixture reacted at 50 °C. In this case, the reaction flask was maintained at the same temperature without further heating or cooling during the aging process. Off-white powders were obtained by adding anhydrous methanol to the flask containing the colloidal product at ambient temperature, which was followed by multiple centrifuging, filtering, and vacuum drying. 0.001 g of the powders were taken from each sample and redispersed in 1 mL of a methylene chloride solution for the UV/Vis and solution PL spectroscopic analyses. Each reaction was repeated more than three times to confirm reproducibility. The samples used for HR-TEM analyses were prepared by placing a drop of the colloidal solution onto a copper grid followed by drying overnight in a high-vacuum oven.

The PL efficiency of the ZnS:Mn nanocrstals were measured and calculated using the method reported by Williams *et al.*[9] This method involves calculating the relative quantum yield through a comparison with a standard material, 0.1 M solution of quinine sulfate in H_2SO_4 (Fluka), whose emission wavelength and absolute quantum yield were reported to be 550 nm and 54.6% (at 22 °C) respectively.[10] Table 1 shows the spectral and physical data of the products obtained.

Results and Discussions

Figure 1 shows HR-TEM images of the ZnS:Mn nanocrystals reacted at four different temperatures. Indeed, the

Table 1. Data summary for the ZnS:Mn nanocrystals reacted at various temperatures

	ZnS:Mn (50)	ZnS:Mn (100)	ZnS:Mn (135)	ZnS:Mn (150)
UV/Vis (λ_{max}, nm)	309	285	309	313
PL emission wavelength (nm)	571	577	570	572
PL efficiency (%)	5.04	6.33	16.20	5.52
HR-TEM image (average particle size, nm)	3.0 (dot)	18.5×2.8 nm^2 (rod) 10 (dot)	9.4×3.8 nm^2 (rod) 18 (dot)	4.0 (dot)

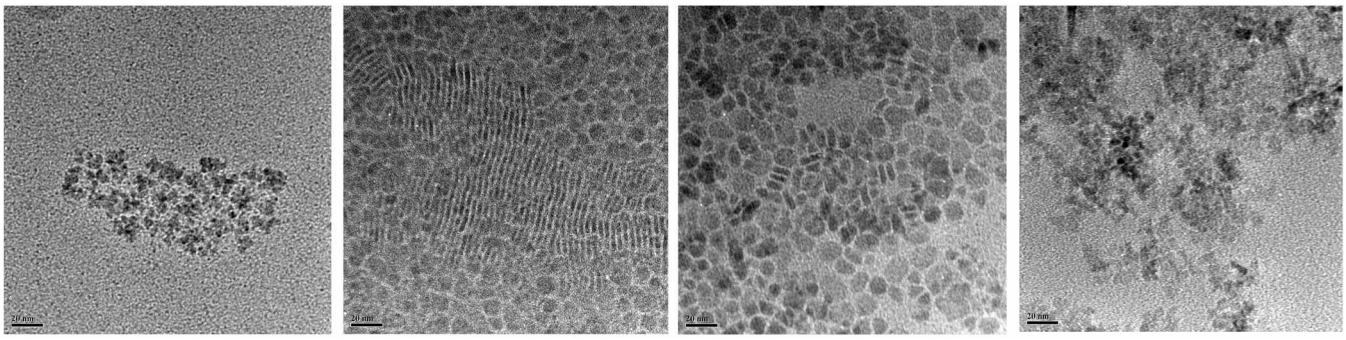

Figure 1. HR-TEM images of ZnS:Mn nanocrystals obtained at (a) 50 °C, (b) 100 °C, (c) 135 °C, (d) 150 °C respectively, the scale bars represent 20 nm.

initial intention was to synthesize the ZnS:Mn nanocrystals at 135 °C (c) because previous work reported that this reaction temperature was the best condition for undoped ZnS nanocrystal formation *via* an organometallic route.[11] However, a mixture of rod-(approximately 9.4 × 3.8 nm^2 size) and dot-(18 nm diameter in average) shaped ZnS:Mn nanocrystals was obtained at this temperature. Therefore, the same reactions were carried out at different temperatures to determine if other types of nanocrystal products could be produced at the corresponding reaction temperatures. As a result, a mixture of longer rods (18.5 × 2.8 nm^2) and smaller dots (10 nm diameter) of ZnS:Mn nanocrystals was obtained from the batch reacted at 100 °C (b). Interestingly, there were no rod-shaped nanocrystals in the samples obtained at 50 °C (a) and 150 °C (d). Instead, monodispersed dots (3-4 nm in diameter) that were smaller than those obtained from the (b) and (c) samples were formed. From these images, it is obvious that the particle sizes for the dots were much larger for samples (b) and (c) than for (a) and (d). These larger dots are probably intermediate forms between rods and dots because they appeared only in the mixture at 135 and 150 °C. In those figures, there was little agglomeration between the particles due to solvent evaporation during sample preparation. However, the appearance of distinct lattice planes in the HR-TEM image with an approximate 5 Å lattice spacing indicate that all nanocrystalline solid samples were made from single crystals rather than polycrystalline aggregates. Unfortunately, a clearer image could not be obtained due to the solvent evaporation and decomposition of the nanocrystals during the HR-TEM observations.

It was reported that MnS and PbS nanocrystals can form two different shapes: rods and polyhedrons. Moreover, these shapes are affected mainly by the crystal growth temperature: the rod shapes are formed at lower temperatures while polyhedrons are formed at higher temperatures.[12] Therefore, the anisotropic rod shape is kinetically favored and the isotropic polyhedral or spherical shapes are thermodynamically favored. In our case, the samples for (b) and (c) also showed a similar pattern in that longer rods and smaller dots were obtained at the relatively lower temperature of 100 °C than at 135 °C. However, only zero dimensional dots were obtained at 50 °C. This is might due to the reaction temperature being too low to allow the formation or growth of rod-shaped nanocrystals. It should be noted that it is rare for nanocrystals to form *via* an organometallic thermal decomposition reaction at this temperature.[13]

Figure 2 shows the spectroscopic data obtained for the ZnS:Mn nanocrystals. The UV/Vis absorption spectra 2-(a) showed broad absorption peaks with the maxima located from 285 to 313 nm. It should be noted that the ZnS:Mn nanocrystals reacted at 100 °C to form a mixture of rods and dots, and showed an approximately 25 nm blue shift in the absorption peak compared with the other samples. A similar phenomenon was observed for GaP nanocrystals in that the absorption spectra for the dots and rods showed corresponding band gaps of 3.48 and 3.46 eV respectively.[14] The solution PL spectra 2-(b) obtained from the ZnS:Mn nanocrystals showed broad emission peaks from 571 to 575 nm. The emission spectra were obtained by fixing the excitation wavelengths of the light source to the corresponding UV/Vis absorption peak positions. From the spectra, it can be seen that the sample prepared at 100 °C showed the largest Stoke shift between the absorption and emission wavelengths. This is because the rod type parent crystal can better trap charge carriers at the surface defects that lie in the band gap states.[15] The calculated relative PL efficiencies at 50, 100, 135 and 150 °C were 5.04%, 6.33%, 16.20%, and 5.52%, respectively. Since the samples were a mixture of rods and dots, their corresponding optical properties could not be separated. There are no reports directly comparing the PL efficiencies of dot and rod shaped nanocrystals. However, it was observed that the emission peaks for the dots (the green and black lines) showed similar intensities, while that for the rod-dot mixtures (the red and blue lines) were significantly different. The former case is probably due to the similar shapes and particle sizes between the two samples. However, in the latter case, the longer and the better shaped rod mixture (135 °C sample) showed much higher PL intensity than that the sample reacted at 100 °C. A similar phenomenon was observed for CdS nanorods in that the longer rods showed a higher PL intensity due to the slower relaxation of the excited state carriers.[15] Moreover, the best PL efficiency was obtained from the sample reacted at 135

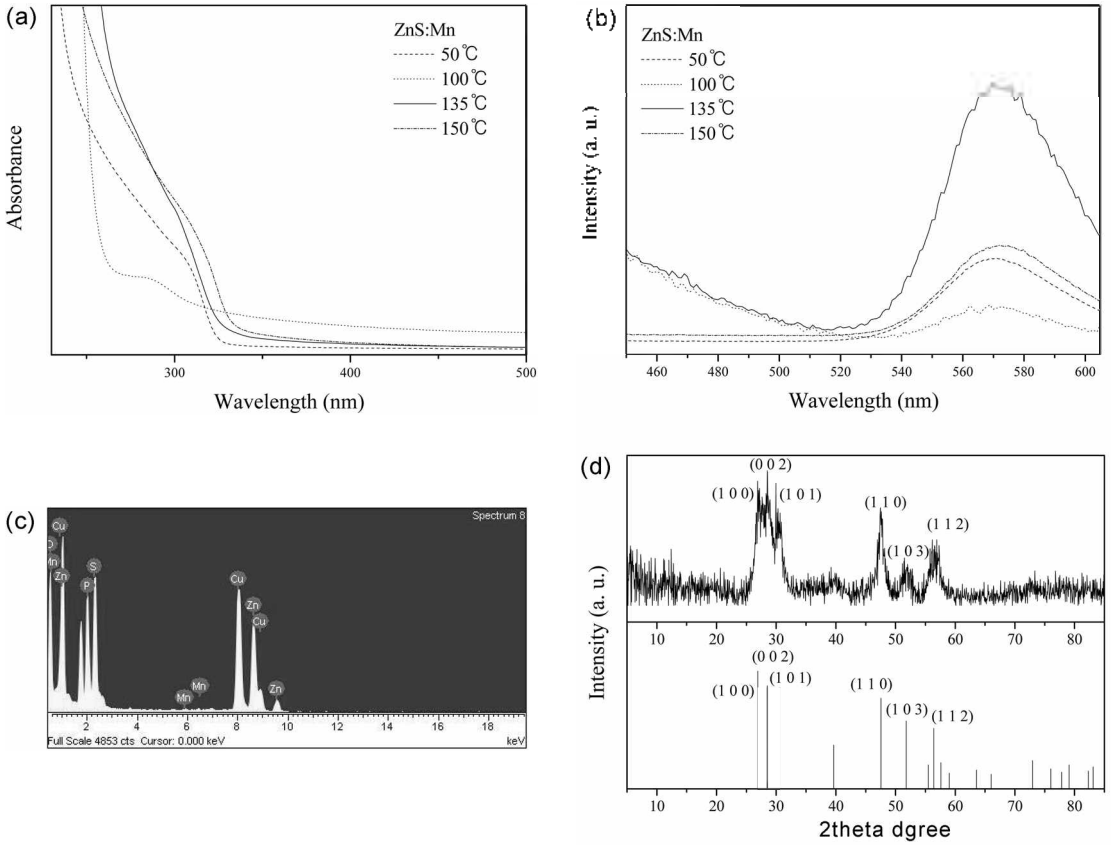

Figure 2. Spectroscopic data for ZnS:Mn nanocrystals; (a) UV/Vis absorptions, (b) PL emissions, (c) EDXS, (C) XRD diagrams. (a) UV/Vis absorption spectra. (a) UV/Vis absorption spectra. (b) PL emissions diagram, the excitation wave lengths were fixed at corresponding UV/Vis absorption maxima. (c) a representative EDXS diagram of the ZnS:Mn (50 °C) nanocrystal. (d) XRD pattern diagrams; a representative diagram for the ZnS:Mn (50 °C) nanocrystal (above), and bulk ZnS solid in a Wurtzite phase with a space group of $P6_3mc$ (below).

°C. This is relevant to the previously mentioned experimental results in that the optimal ZnS nanocrystal formation conditions were observed at this temperature.[11] Figure 2-(c) shows the energy dispersive X-ray spectroscopy (EDXS) diagram to confirm the formation of ZnS:Mn nanocrystals in the solid state. EDXS elemental analysis also showed that the doping concentration of manganese (II) ions in the ZnS:Mn nanocrystals synthesized at 50°, 100°, 135° and 150 °C were 2.98%, 0.74%, 1.03%, and 0.78%, respectively. The manganese ion doping concentration of the ZnS:Mn crystals were originally aimed at approximately 1-2% because it was shown that the best PL efficiency was observed in this range.[17] It was reported that the dopant concentration affects the emission wavelength and peak intensities of the bulk ZnS:Mn solid by changing the band gap energy and quantum yield.[18] However, in our case, the effect of the dopant concentration was not so significant due to the similar emission wavelengths for the ZnS:Mn nanocrystals, particularly with sample (a), which contained a much higher doping concentration (2.98%) than the other samples.

Finally, the wide angle X-ray diffraction (XRD) patterns of the ZnS:Mn nanocrystal 2-(d) showed some obviously indexable peaks, such as the (110), (002), (101), (103) and (112) planes, which indicates that the ZnS:Mn nanocrystals possess a Wurtzeite crystalline phase in the $P6_3mc$ space group.[19] In addition, the average crystallite size of 4.2 nm, which was calculated using the Debye-Scherrer formula.[20] is also in good agreement with that obtained from the HR-EM images. The EDXS and XRD diagrams showed are for the ZnS:Mn nanocrystal sample reacted at 50 °C only but the data from the other samples was similar.

Conclusion

ZnS:Mn nanocrystals with two different shapes at were obtained under different reaction conditions. Only zero-dimensional dot shaped ZnS:Mn nanocrystals were formed at lower and higher reaction temperatures (50 and 150 °C), while mixtures of dots and rods were obtained at 100 and 135 °C. The sizes of the dots were larger for the samples synthesized at intermediate temperatures, and longer rods were formed at 100 °C than at 135 °C. In addition, ZnS:Mn nanocrystals can be formed from an organometallic decomposition reaction at unusually low reaction temperatures (50 °C).

Acknowledgment. This study was supported by *Dankook University Faculty Research Fund 2006.*

References

1. (a) Markovich, G. C.; Collier, P.; Henrichs, S. E.; Remacle, F.; Levine, R. D.; Heath, J. R. *Acc. Chem. Res.* **1999**, *32*, 415. (b) Alivisatos, A. P. *Science* **1996**, *271*, 933.
2. Brus, L. E. *Appl. Phys. A: Solid Surf.* **1991**, *53*, 465.
3. Gaetzel, M. *Plat. Met. Rev.* **1994**, *38*, 151.
4. Jun, Y. W.; Jang, J. T.; Cheon, J. *Bull. Kor. Chem. Soc.* **2006**, *27*, 961.
5. Law, M.; Goldberger, J.; Yang, P. *Annu. Rev. Mater. Res.* **2004**, *34*, 83.
6. Hu, J.; Odom, T. W.; Lieber, C. M. *Acc. Chem. Res.* **1999**, *32*, 435.
7. Hwang, J. M.; Oh, M. O.; Kim, I.; Lee, J. K.; Ha, C.-S. *Curr. Appl. Phys.* **2005**, *5*, 31.
8. (a) Hwang, C.-S.; Lee, N. R.; Kim, Y. A.; Park, Y. B. *Bull. Kor. Chem. Soc.* **2006**, *27*, 1809. (b) Lee, J. H.; Kim, Y. A.; Kim, K. M.; Huh, Y. D.; Hyun, J. W.; Kim, H. S.; Noh, S. J.; Hwang, C.-S. *Bull. Kor. Chem. Soc.* **2007**, *28*, 1091.
9. Williams, A. T. R.; Winfield, S. A.; Miller, J. N. *Analyst* **1983**, *108*, 1067.
10. Melhuish, W. H. *J. Phys. Chem.* **1961**, *65*, 229.
11. Hwang, C.-S.; Cho, I. H. *Bull. Kor. Chem. Soc.* **2005**, *26*, 1776.
12. Kim, Y. H.; Jun, Y.; Jun, B. H.; Lee, S. M.; Cheon, J. W. *J. Am. Chem. Soc.* **2002**, *124*, 13656.
13. Ozin, G.; Arsenault, A. C. *Nanochemistry*; RSC publishing: U. K., 2005; Ch. 5.
14. Hu, J.; Li, L. S.; Yang, W.; Manna, L.; Wang, L.; Alivisatos, A. P. *Science* **2001**, *292*, 2060.
15. Tata, M.; Banerjee, S.; John, V. T.; Waguespack, Y.; Mcpherson, G. *Coll. Surf. A Phys. Chem. and Eng. Asp.* **1997**, *127*, 39.
16. Sarcar, R.; Shaw, A. K.; Narayanan, S. S.; Rothe, C.; Hintschich, S.; Monkman, A.; Pal, S. K. *Opt. Mater.* **2007**, *29*, 1310.
17. Yi, G.; Sun, B.; Yang, F.; Chen, D. *J. Mater. Chem.* **2001**, *11*, 2928.
18. Warren, A. J.; Thomas, C. B.; Stevens, P. R. *Appl. Phys.* **1983**, *16*, 225.
19. Zhuang, J.; Zhang, X.; Wang, G.; Li, D.; Yang, W.; Li, T. *J. Mater. Chem.* **2003**, *13*, 1853.
20. *International Union of Crystallography* in *International Tables for X-ray Crystallography, Part III*; Netherlands, Dordrecht, 1985; p 318.